

## Supporting Information

### **Versatile “on-off” biosensing of thrombin and miRNA based on Ag (I) ion-enhanced or Ag nanocluster-quenched electrochemiluminescence coupled with hybridization chain reaction amplification**

Junjun Ge, Chunli Li, Yu Zhao, Xijuan Yu, Guifen Jie\*

*Key Laboratory of Optic-electric Sensing and Analytical Chemistry for Life Science, MOE; Shandong Key Laboratory of Biochemical Analysis; Key Laboratory of Analytical Chemistry for Life Science in Universities of Shandong; College of Chemistry and Molecular Engineering, Qingdao University of Science and Technology, Qingdao 266042, PR China*

#### **Table of Contents**

<b>EXPERIMENTAL SECTION</b> .....	S-2
<b>RESULTS AND DISCUSSION</b> .....	S-7
<b>REFERENCES</b> .....	S-15

## EXPERIMENTAL SECTION

**Table 1.** Sequences of DNA and RNA used in this work

Oligonucleotide	Sequence (5' →3' )
H1	HS-GTC AGT GAG CTA GGT <u>TAG ATG TCG</u> CCA TGT GTA GAC GAC ATC TAA CCT AGC
H2	CCT CCT TCC TCC AAT AGA CGA CAT CTA ACC TCA AGT TAA GCT AGG TTA GAT GTC GTC TAC ACA TGG
H3	AAC TTG AGG TTA GAT GTC GTC TAA ACC ATG TGT AGA CGA CAT CTA ACC TAG CTT TTT TTT TTT T-NH <sub>2</sub>
P1	GGT TGG TGT GGT TGG (T) <sub>15</sub> CGT CTA CAC ATG GCG ACA TCT A
P2	AGT CCG TGG TAG GGC AGG TTG GGT GAC T(T) <sub>15</sub> CGT CTA CAC ATG GCG ACA TCT A
CsDNA	TCA ACA TCA GTC TGA TAA GCT A
MiRNA-21	UAG CUU AUC AGA CUG AUG UUG A

The red underline is the complementary pairing of the stems inside the hairpin. Blue is the part of the molecular biped machine paired with the hairpin. Gray is the two aptamers of thrombin. Yellow and green are the parts that are paired between the cards.

**Chemicals and Materials.** Thrombin was purchased from Sigma Aldrich. Trichloroauric acid trihydrate (49.0%, H<sub>2</sub>Cl<sub>4</sub>.3H<sub>2</sub>O) was purchased from Alfa Aesar (Tianjin) Chemical Co., Ltd. Sodium citrate (>99.0%), selenium powder (99.9%), Silver nitrate and sodium borohydride were purchased from Qingdao Zhengye Reagent Instrument

Co. Ltd. Mercaptopropionic acid (98.0%, MPA), Mercaptohexanol (98.0%, MCH), Tetraethoxysilane (98.0%, TEOS) and cetyltrimethylammonium bromide (CTAB) were purchased from Aladdin Reagent (Shanghai) Co., Ltd. Poly (diallyldimethylammonium chloride) (PDDA, 20%, w/w, in water, MW = 200,000–350,000) was from Sigma–Aldrich. Ethidium bromide was purchased from Shanghai Civic Technology Co., Ltd. CdCl<sub>2</sub>·2.5H<sub>2</sub>O (98.0%) were purchased from Shanghai Runjie Chemical Reagent Co., Ltd. All the DNA and RNA sequences were synthesized and purified by Sangon Biotech (Shanghai) Co., Ltd. The DNA and RNA sequences used in this work are listed in Table 1.

**Apparatus.** Transmission electron microscopy (TEM) images were recorded on a JEOL JEM-2100EX transmission electron microscope (Japan). Atomic force microscope (AFM) images were recorded on a Dimension FastScan<sup>TM</sup> Atomic force microscope (Bruker AXS GmbH, Germany). UV-vis absorption spectra were measured with Lambda 35 UV-Vis-NIR spectrophotometer (US PerkinElmer Instrument Co., Ltd.). Fluorescence measurements were performed on a F-4500 fluorescence spectrometer (Japan). ECL detection experiments were carried out on MPI-E ECL analyzer (Remex Electronic Instrument Lt. Co., Xi'an, China) with three-electrode system containing a Pt wire counter electrode, saturated calomel (saturated KCl) reference electrode, and a gold working electrode. Cyclic voltammetry (CV) and Electrochemical impedance spectroscopy (EIS) were measured on CHI 660E Electrochemical Workstation (Chenhua Instrument Co., Ltd. Shanghai, China).

**DNA and TB treatment.** All DNA and TB were dissolved in Tris-HCl buffer solution (pH=7.4, 20 mM) containing 5 mM KCl, 140 mM NaCl and 2 mM MgCl<sub>2</sub>. H1, H2 (1 μM), H3 (10 μM) were annealed at 95 °C for 5 min and slowly cooled down to room temperature. Among them, H1 was diluted to 0.3 μM by 1 mM TCEP (dissolve in Tris-HCl) before use.

**Preparation of gold nanoparticles (Au NPs).** The colloidal AuNPs with 15 nm diameter were prepared from  $\text{HAuCl}_4$  aqueous solution and sodium citrate according to the previous protocol.<sup>1</sup> Briefly, 1 mL of 1%  $\text{HAuCl}_4$  solution was added to 49 mL of boiling deionized water in three-necked flask. 2 mL of 2 wt% sodium citrate was added immediately and the mixture was stirred for 15 min until the color turned watermelon-red. The heating was stopped and the final product was naturally cooled to room temperature and stored at 4 °C until use.

**Preparation of CdSe QDs.** Mercaptopropionic acid (MPA)-capped CdSe QDs were synthesized using a slightly modified procedure reported previously.<sup>2</sup> 0.75 mM selenium powder and 10 mM  $\text{NaBH}_4$  were dissolved in 5 mL of double-distilled water to form a black mixture, which was stirred under  $\text{N}_2$  atmosphere until it became clear, the  $\text{NaHSe}$  precursor was obtained. After 30 mL of 0.4 mM  $\text{CdCl}_2$  was mixed with 56  $\mu\text{L}$  of MPA, 1 M  $\text{NaOH}$  was added to adjust its pH to 10. The clear solution was bubbled with highly pure  $\text{N}_2$  for 30 min. Then the above two precursors were mixed under  $\text{N}_2$  protection, and heated to boiling with stirring for 2 h. The obtained orange and transparent CdSe colloid was naturally cooled to room temperature and stored at 4 °C.

**Preparation of MSN and PMSN.** MSN was synthesized according to the previously reported method with slight modification.<sup>3</sup> Typically, 250 mg of CTAB and 875  $\mu\text{L}$  of sodium hydroxide (2.0 M) were successively added into 120 mL of ultrapure water under stirring and kept for 20 min at 80 °C. Then, 1.25 mL of TEOS was added to the mixture under continuous stirring for an additional 2 h. The resultant product was obtained by filtration and dried at room temperature, and then refluxed in a mixture of  $\text{HCl}$  and methanol for 10 h to remove the excessive CTAB. The obtained MSN was filtered, washed with ultrapure water and methanol, and then dried at 60 °C.

Next, MSN was positively charged functionalization with PDDA. 16 mg of the as-synthesized MSN was dispersed in 8.0 mL of 1% PDDA salt solution containing 0.02 M NaCl, and then ultrasonicated for 30 min to form a homogeneous suspension of positively charged PDDA-MSN. Afterward, the obtained PDDA-modified MSN (PMSN) was centrifuged (15 000 rpm, 10 min), washed with ultrapure water, and dried at 80 °C.

**Assay of SPCR amplification by Gel Electrophoresis.** Before the gel electrophoresis assay, 23  $\mu\text{L}$  sample (5  $\mu\text{L}$  H1, 5  $\mu\text{L}$  H2, 5  $\mu\text{L}$  H3, 2  $\mu\text{L}$  P1, 2  $\mu\text{L}$  P2, 4  $\mu\text{L}$  TB) were incubated for 1 h at room temperature. Among them, the concentration of H1, H2, H3 was  $10^{-5}$  M, the concentration of P1, P2 was  $10^{-6}$  M and the concentration of TB was  $10^{-10}$  M. The sample and 2  $\mu\text{M}$  H1, H2, H3 were then put on a polyacrylamide gel. The electrophoresis was carried in 1 $\times$ tris-acetic acid-EDTA (TAE) (pH 8.0) at 180 V constant voltages for 3 min and 135 V for 1.5 h. After EB staining, the gel was scanned using the Gel imaging analyzer (Saizhi Venture Technology Co., Ltd. Beijing, China).

**Preparation of H3-CdSe QDs.** After 20  $\mu\text{L}$  of 0.1 M EDC (1-(3-Dimethylaminopropyl)-3-ethylcarbodiimide hydrochloride) and 20  $\mu\text{L}$  of 0.025 M NHS (N-Hydroxysuccinimide; 1-hydroxypyrrolidine-2,5-dione) were added to 200  $\mu\text{L}$  of CdSe QDs for activating 1 h at room temperature, 20  $\mu\text{L}$  of  $10^{-5}$  M H3 was added to link with the QDs at 37 °C for 5 h, and then redispersed in ultrapure water.

**Construction of the ECL Biosensor for TB detection.** After 10  $\mu\text{L}$  of H1 (0.3  $\mu\text{M}$ ) was dropped on the electrode surface modified with gold nanoparticles, and incubated at 37 °C for 12 h, 8  $\mu\text{L}$  of mercaptohexanol (MCH, 1 mM) was dropped on the electrode to incubate for 1 h. Prior to measurement, a mixture of 70 nM P1, 70 nM P2, 0.35  $\mu\text{M}$  H2, 0.35  $\mu\text{M}$  H3-CdSe QDs and various concentrations of thrombin in Tris-HCl buffer was

prepared and incubated for 1 h at room temperature. 10  $\mu\text{L}$  of the mixture was dropped on the electrode surface to incubate for 80 min at room temperature. After the electrode was washed with PBS, 10  $\mu\text{L}$  of  $\text{AgNO}_3$  solution (1 mM) was dropped on the above electrode surface for 60 min to obtain the finished biosensor for TB detection.

**Construction of the ECL Biosensors for detection miRNA-21.** The first part of the ECL biosensor (AE/AuNPs/H1/MCH/TB-P1-P2-H2-H3-CdSe) was similar to that for detecting TB, except that the TB concentration was fixed at 10 nM.

10.0 mg of the prepared PMSN was suspended into 600  $\mu\text{L}$  of 20 mM  $\text{AgNO}_3$  solution, and then the mixture was gently shaken at room temperature overnight. Subsequently, 10  $\mu\text{L}$  of 2 nM CsDNA was incubated with PMSN/ $\text{AgNO}_3$  at room temperature for 4 h under gentle stirring. The mixture was then centrifuged (3000 rpm, 2 min) and resuspended into 1.0 mL Tris-HCl buffer. Then, miRNA-21 with different concentrations was added and incubated at 37  $^\circ\text{C}$  for 2 h. After centrifugation, 10  $\mu\text{L}$  of supernatant was dropped onto the prepared ECL biosensor to react 30 min at 4  $^\circ\text{C}$ , then 10  $\mu\text{L}$  of 1 mM  $\text{NaBH}_4$  was added dropwise to the electrode and allowed to react overnight at 4  $^\circ\text{C}$ . Finally, ECL measurements were detected by a MPI-E ECL analyzer in 3 mL pH 7.4 PBS (0.1 M) containing  $\text{S}_2\text{O}_8^{2-}$  (0.05 M) and KCl (0.1 M).

**Determination of Thrombin in Human Serum.** The fresh human serum samples were supplied by the Affiliated Hospital of Qingdao University. ECL responses of pure serum and standard-added serum were determined with the prepared biosensor. The thrombin content in serum was derived from the standard curve and the regression equation.

**Determination of miRNA-21 in Human Serum.** For the purpose of quantifying miRNA in human plasma, human blood was obtained from healthy, lung cancer, and breast cancer volunteers (provided by the Affiliated Hospital of Qingdao University). Afterward,

the same procedure as mentioned above is performed for miRNA-21 detection.

## RESULTS AND DISCUSSION

**Characterization of Au NPs.** The Au NPs used for the biosensor were characterized by transmission electron microscopy (TEM) image (Figure S1A), the particles with average diameter of about 15 nm were uniformly distributed. The UV-vis spectrum of the Au NPs shows a strong absorption band at 522 nm (Figure S1B), indicating the formation of the Au NPs.

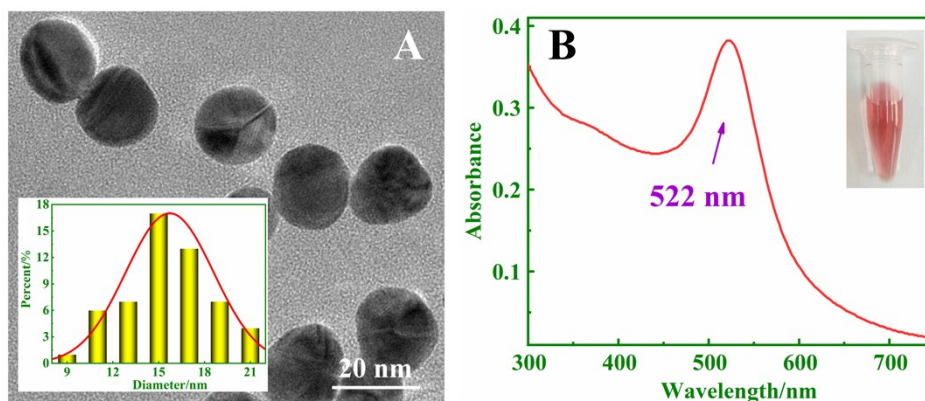


**Figure S1.** (A) TEM image of Au NPs (inset: size distribution of Au NPs). (B) UV-vis absorption of Au NPs.

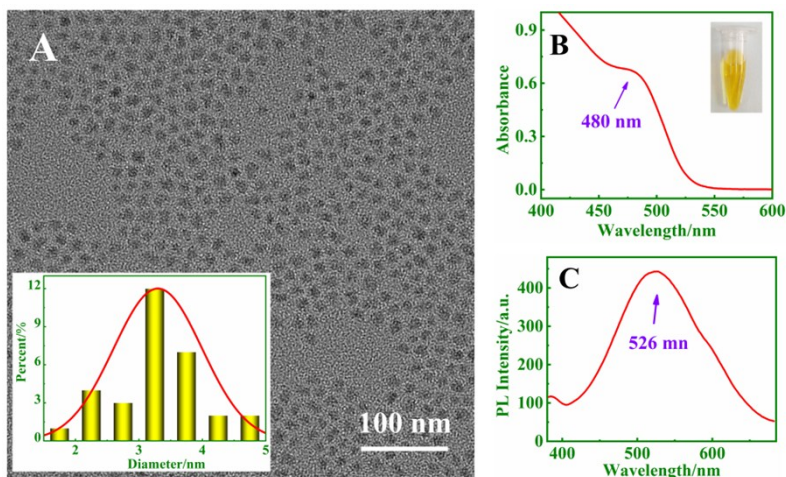


**Figure S2.** (A) TEM image of CdSe QDs (inset: size distribution of CdSe QDs). (B) UV-vis absorption of CdSe QDs. (C) PL emission spectrum of CdSe QDs.

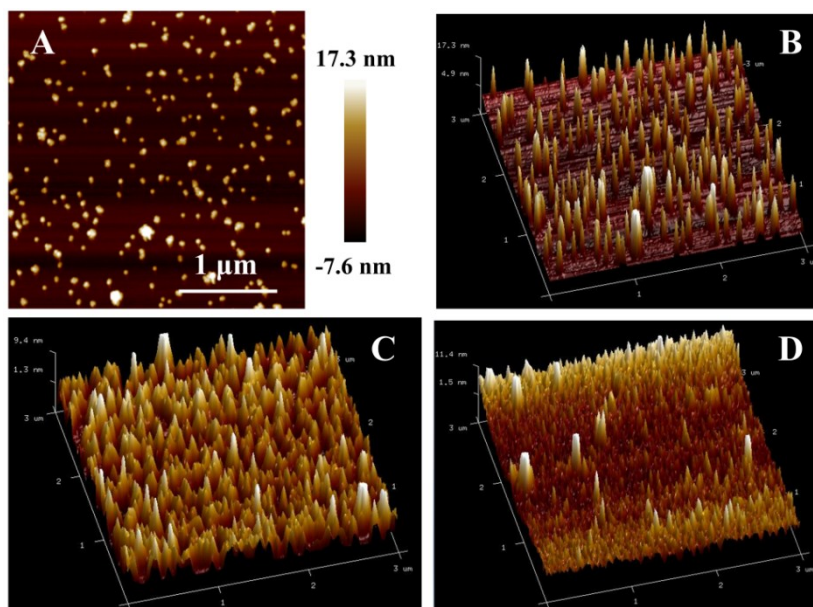


**Figure S3.** AFM images of Au electrode at different stages: (A) the Au NPs surface (2D), (B) the Au NPs surface(3D), (C) the CdSe QDs + Au NPs surface, (D) the CdSe QDs + Au NPs + Ag NCs surface.

**Signal Intensity and Stability of CdSe QDs.** The ECL properties of CdSe QDs on the electrode were characterized. Figure S4A is the ECL–potential curve of CdSe QDs, a strong ECL peak at -1.495 V was observed, indicating that the synthesized CdSe QDs possess good ECL performance. The ECL was generated from the reaction of CdSe QDs with  $S_2O_8^{2-}$ , the possible ECL mechanisms are as follows.<sup>4</sup>

- (1)  $CdSe + e^- \rightarrow CdSe^{\cdot-}$
- (2)  $S_2O_8^{2-} + e^- \rightarrow SO_4^{2-} + SO_4^{\cdot-}$
- (3)  $CdSe^{\cdot-} + SO_4^{\cdot-} \rightarrow CdSe^* + SO_4^{2-}$
- (4)  $CdSe^* \rightarrow CdSe + h\nu$

Figure S4(B) shows the ECL signals of the CdSe QDs on the Au electrode under continuous potential scanning, the high and stable ECL indicates that CdSe QDs can be used to construct ECL biosensor for detection of TB and miRNA-21.



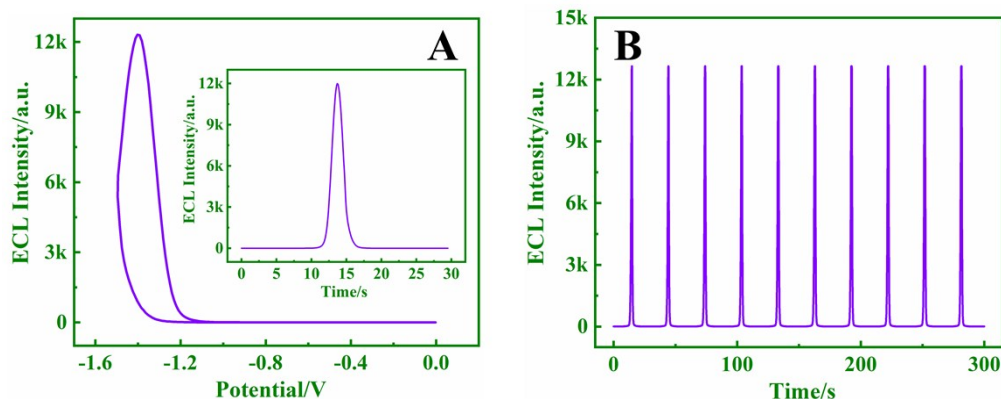


**Figure S4.** (A) ECL intensity-potential curve of CdSe QDs, inset: ECL intensity-time curve of CdSe QDs. (B) ECL emission under continuous cyclic potential scan for 10 cycles. (PMT=-600V).

### Feasibility of the ECL Biosensor for Detection of TB and miRNA-21.

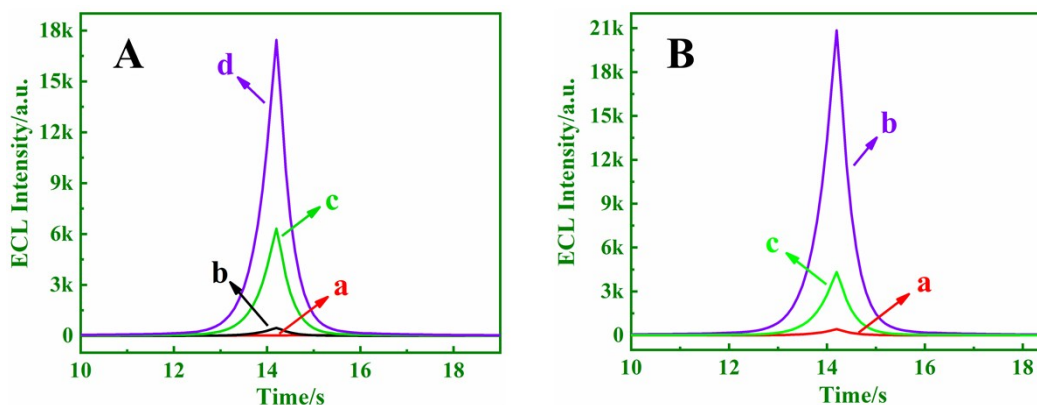


**Figure S5.** ECL signals of the modified electrodes under different conditions. (A) “signal on” biosensor for TB detection (PTM=-800, TB concentration: 10 pM): bare gold electrode (curve a), in the absence of TB (curve b), in the presence of TB (curve c), in the presence of  $\text{Ag}^+$  (curve d); (B) “signal off” biosensor for miRNA-21 detection (PTM=-900, TB concentration: 10 pM, RNA concentration: 0.1 pM): bare gold electrode (curve a), in the absence of target miRNA-21 (curve b), in the presence of target miRNA-21 (curve c). ECL was performed in pH 7.4 PBS (0.1 M) containing  $\text{S}_2\text{O}_8^{2-}$  (0.05 M) and KCl (0.1 M).

In addition, the “signal off” biosensing process for miRNA-21 was characterized. Figure S5B showed that bare electrode has no ECL peak (curve a). In the absence of target miRNA-21, ECL was the same as curve c in Figure S5A. In order to observe the quenched

ECL signal more obviously, the photomultiplier tube was adjusted to -900 V, ECL signal in curve b was about 3.07 times of curve c in Figure S5A by calculation ( $6798 \times 3.07 = 20851$  a.u.). In the presence of miRNA-21, the released  $\text{AgNO}_3$  from PMSN to C-rich DNA were in situ reduced to Ag NCs by  $\text{NaBH}_4$ , so ECL energy transfer from CdSe QDs to Ag NCs and consumption of coreactant  $\text{S}_2\text{O}_8^{2-}$  by Ag NCs double quenched QDs ECL, resulting in significant decrease of ECL signal (curve c), which can be used for miRNA-21 detection.

**Optimization of Experimental Conditions.** To achieve the best performance of the ECL biosensor, the experimental parameters were optimized. The effect of H1 density on the electrode for ECL was studied. Too low or high H1 density may inhibit ECL due to the incomplete hybridization reaction or steric hindrance (Figure S6A), the highest ECL was obtained at  $0.3 \mu\text{M}$  H1, this was selected as the optimized concentration.

In principle, BMM can open H1 on the electrode to link H2/H3-CdSe QDs in long reaction time, so the time of BMM-powered SPCR was investigated. As shown in Figure S6B, the signal response increased with the prolonging of reaction time and reached a plateau after incubation for 80 min. Therefore, a reaction time of 80 min was chosen for BMM-powered SPCR.

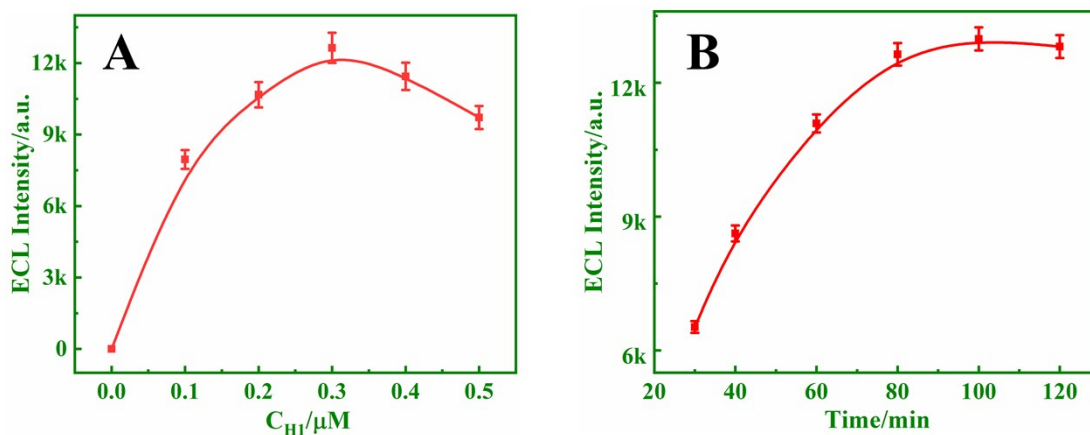


**Figure S6.** Effects of (A) H1 concentration, (B) reaction time of SPCR on ECL responses of the

biosensor. TB concentration:  $10^{-1}$  nM.

The effect of  $\text{AgNO}_3$  concentration in PMSN on ECL is studied, ECL signal decreased with increasing  $\text{AgNO}_3$  concentration until it is low enough at 20 mM  $\text{AgNO}_3$  (Figure S7A), so 20 mM  $\text{AgNO}_3$  was used for detection. The signal response decreased with the increase of CsDNA concentration, and reached a plateau in 2 nM (Figure S7B). Similarly, ECL signal decreased with increasing hybridization reaction time of target miRNA-21, and became stable after 2 h, so 2 h was chosen for reaction (Figure S6C).

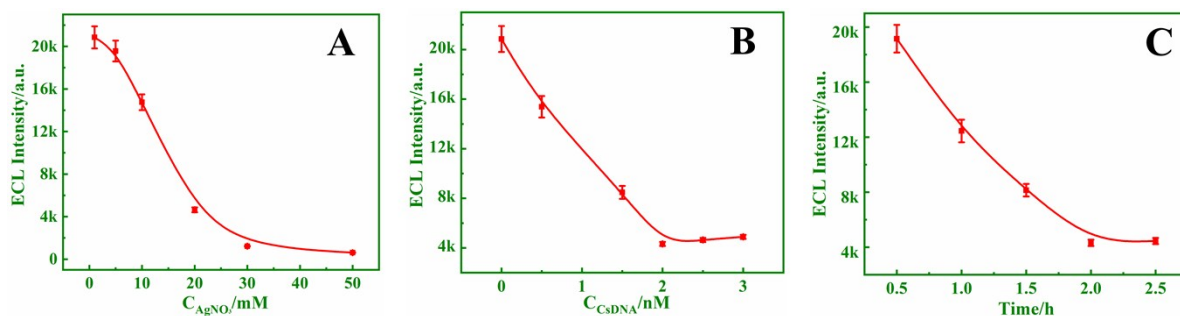


**Figure S7.** Effects of (A) concentration of  $\text{AgNO}_3$ , (B) concentration of CsDNA, (C) reaction time of target miRNA-21 on ECL responses of the biosensor. TB concentration: 10 nM; miRNA-21 concentration in: 100 pM.

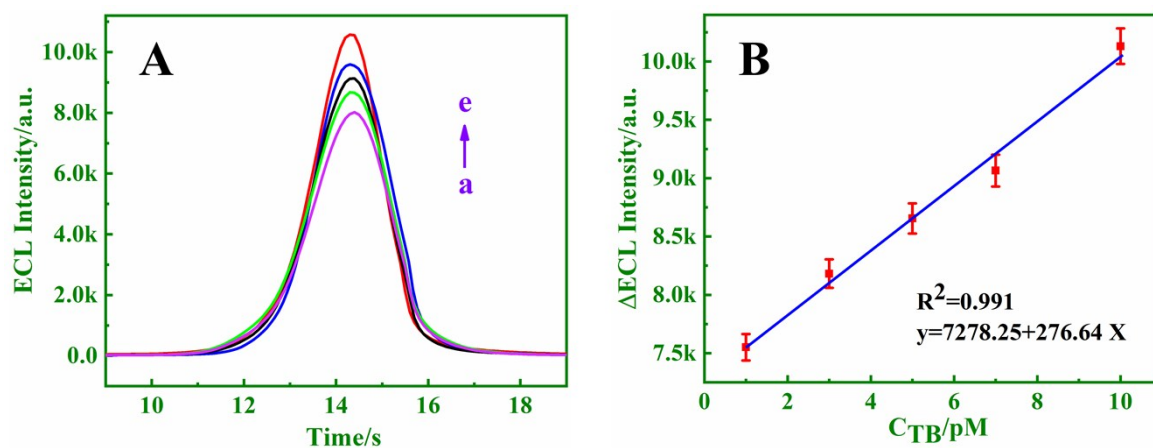


**Figure S8.** (A) ECL responses of the biosensor for different concentrations of TB (pM). (a) 1, (b) 3, (c) 5, (d) 7, (e) 10. (B) Relationship between ECL responses and concentration of TB, inset: the logarithmic calibration curve for TB detection. (PMT=-800).

**ECL Detection of TB.** Detection of thrombin in the picomolar concentration range of blood is of great importance to clinical diagnosis. The ECL-concentration relationship in the picomolar range was further studied in Figure S8A. A linear relationship between  $\Delta$ ECL signals and the concentrations of TB was obtained in the range from 1 to 10 pM ( $R^2 = 0.991$ ) (Figure S8B). This demonstrates that the proposed ECL sensor can be employed for TB detection.

**Selectivity of the ECL Biosensor.** In addition, the specificity of the method for detecting miRNA-21 miRNA-141 was studied. As can be seen from Figure S9B, there was no significant change in the ECL responses in detecting miRNA-141, miRNA-143, and miRNA-155 in comparison with the blank. In contrast, obvious changes of ECL responses were observed when miRNA-21 ( $10^2$  pM) was detected, which suggest that the method has good specificity for miRNA-21 assay.

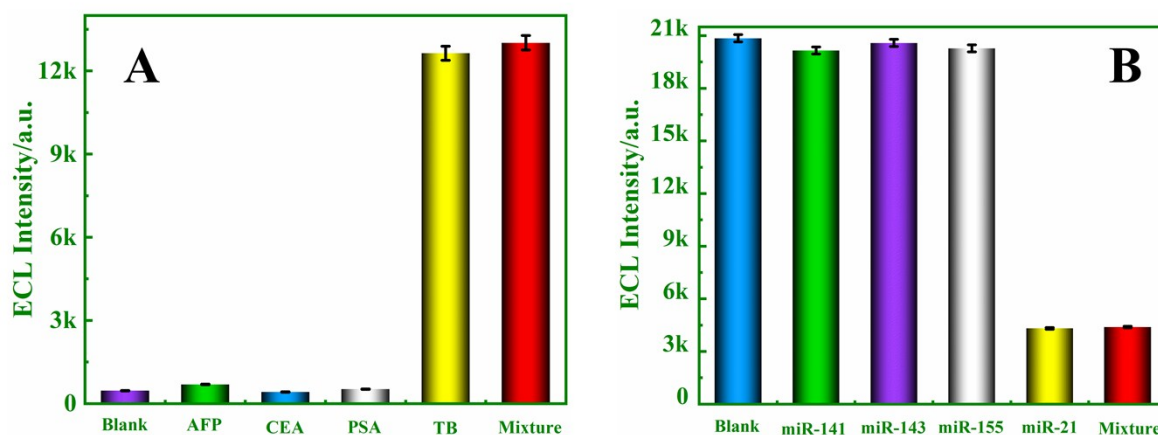


**Figure S9.** (A) Selectivity of the ECL biosensor for TB assay by comparison with AFP, CEA, PSA at the same concentration of 100 pM and blank (in absence of TB). (B) Specificity of the ECL biosensor for target miRNA-21 assay by comparison with miRNA-141, miRNA-143, miRNA-155 at 100 pM, the mixture (miRNA-141:miRNA-143:miRNA-155:miRNA-21=1:1:1:1) and blank (in absence of miRNA-21).

**Comparison of the proposed biosensor with other reported Methods for TB and MiRNA-21 Determination.** Table S1 and Table S2 summarized some of the commonly applied methods for determination of TB and miRNA, respectively. It is noticeable that the present ECL biosensors offer favorable detection sensitivity, which is greatly important for practical applications in the assay of real biological samples.

**Table S1. Comparison of Different Methods for TB Determination**

Detection techniques	Linear range	LOD	refs
DPV	2 pM - 20 nM	0.76 pM	(5)
colorimetric	13 fM - 0.13 nM	5 fM	(6)
ECL	0.90pM - 226pM	0.4 pM	(7)
DPV	0.1pM - 10 pM	56 fM	(8)
ECL	1fM -10 nM	0.165 fM	This work

**Table S2. Comparison of Different Methods for Assay of MiRNA-21**

Detection techniques	Linear range	LOD	refs
ECL	0.1 fM-100pM	22 aM	(9)
Raman	1 fM-100 pM	393 aM	(10)
fluorescence	100 fM to 10 nM	58 fM	(11)
ECL	10 aM - 1.0 pM	3.3 aM	(12)
PEC	5 fM-5 pM	1.67 fM	(13)
ECL	10 aM - 1 nM	4.97aM	This work

**Application of the Proposed Method in Real Sample Analysis.** To further evaluate the detecting ability of the ECL biosensor for thrombin in complex biological matrixes, we

applied the method to the assay of human serum samples. The recoveries of the samples (in the range 99.98–106.1%) and the relative standard deviation (RSD) values (less than 4.7%) were summarized in Table S3, which indicated that the accuracy and precision of the proposed method were satisfactory in human serum, and has the potential to be applied in clinical thrombin determination.

**Table S3. Results for Thrombin Determination in Diluted Serum Samples**

sample	Added (pM)	Found (pM)	Recovery (%)	RSD (% ,n=3)
1	0	0.055		3.2
2	2	2.052	99.98	4.7
3	4	4.299	106.10	3.6
4	8	8.142	101.08	4.4

**Table S4. Results for miRNA-21 Determination in Diluted Serum Samples**

sample	Found in serum (pM)	Added (pM)	Found (pM)	Recovery (%)	RSD (% ,n=3)
1	0.0134	2	2.045	101.58	1.6
2	0.0134	4	3.914	97.52	3.1
3	0.0134	8	8.161	101.84	2.8
4	4.64	2	6.56	96.00	4.2
5	4.64	4	8.82	104.50	3.5
6	4.64	8	12.91	103.38	1.9
7	6.18	2	8.23	102.50	2.6
8	6.18	4	10.47	107.25	3.7
9	6.18	8	14.06	98.50	2.3

Human serum samples are also used to validate the practical applicability of the proposed ECL-biosensing method for miRNA-21 assay, the detection results were shown in table S4.

Compared with healthy human serum (samples 1–3), the content of miRNA-21 in lung cancer patient serum (samples 4–6) and breast cancer patient serum (samples 7–9) are dozens of times higher. Furthermore, miRNA-21 with known concentrations was added to those serum samples, the obtained recoveries were between 96.00% and 107.25%. Considering that miRNA-21 is an oncogene and antiapoptotic indicator, the present method is promising for application in early clinical diagnose.

## REFERENCES

- (1) G. F. Jie, J. J. Ge, X. S. Gao and C. L. Li, *Biosens. Bioelectron.*, 2018, **118**, 115–121.
- (2) Q. Kuang, C. C. Li, Z. W. Qiu, S. Y. Niu and T. Y. Huang, *Sensor. Actuat B-Chem.*, 2018, **274**, 116–122.
- (3) P. P. Gai, C. Gu, T. Hou and F. Li, *ACS Appl. Mater. Interfaces.*, 2018, **10**, 9325–9331.
- (4) P. Wu and X. P. Yan, *Chem. Soc. Rev.*, 2013, **42**, 5489–5521.
- (5) A. Chen, S. Ma, Y. Zhuo, Y. Q. Chai and R. Yuan, *Anal. Chem.*, 2016, **88**, 3203–3210.
- (6) C. Y. Song, Y. J. Yang, B. Y. Yang, Y. Z. Sun, Y. P. Zhao and L. H. Wang, *Nanoscale.*, 2016, **8**, 17365–17373.
- (7) L. D. Wang, R. J. Deng and J. H. Li, *Chem. Sci.*, 2015, **6**, 6777–6782.
- (8) A. Chen, G. F. Gui, Y. Zhuo, Y. Q. Chai, Y. Xiang and R. Yuan, *Anal. Chem.*, 2015, **87**, 6328–6334.
- (9) M. Wang, H. Yin, N. Shen, Z. Xu, B. Sun and S. Ai, *Biosens. Bioelectron.*, 2014, **53**, 232–237.
- (10) J. Zhu, H. Gan, J. Wu and H. H. Ju, *Anal. Chem.*, 2018, **90**, 5503–5508.
- (11) J. Li, Y. Jiao, Q. Liu and Z. Chen, *ACS Sustainable Chem. Eng.*, 2018, **6**, 6738–6745.
- (12) X. Y. Wang, A. Gao, C. C. Lu, X. W. He and X. B. Yin, *Biosens. Bioelectron.*, 2013, **48**, 120–125.

(13) C. Zhu, M. Liu, X. Li, X. Zhang, J. Chen, *Chem. Commun.*, 2018, **54**,10359–10362.